Time-reversed lasing in the terahertz range and its preliminary study in sensor applications

Yun Shen [a], Huaqing Liu [a], Xiaohua Deng [b],[*], Guoping Wang [c]

[a] Department of Physics, Nanchang University, Nanchang 330031, China
[b] Institute of Space Science and Technology, Nanchang University, Nanchang 330031, China
[c] Key Laboratory of Artificial Micro- and Nano-Structures of Ministry of Education and School of Physics and Technology, Wuhan University, Wuhan 430072, China

ABSTRACT

Time-reversed lasing in a uniform slab and a grating structure are investigated in the terahertz range. The results show that both the uniform slab and grating can support terahertz time-reversed lasing. Nevertheless, due to the tunable effective refractive index, the grating structure can not only exhibit time-reversed lasing more effectively and flexibly than a uniform slab, but also can realize significant absorption in a broader operating frequency range. Furthermore, applications of terahertz time-reversed lasing for novel concentration/thickness sensors are preliminarily studied in a single-channel coherent perfect absorber system.

© 2016 Elsevier B.V. All rights reserved.

1. Introduction

Time-reversed lasing has attracted much attention due to its widely potential applications in modulators, detectors, phase controlled optical switches, etc. [1–4]. To achieve time-reversed lasing, resonator systems consisting of media with particular degree dissipation and termed "coherent perfect absorbers (CPAs)" are investigated. Since the detailed theory investigation of CPA were first specifically illustrated by Chong et al. [5], and the two-channel CPA in silicon slab was experimentally demonstrated by Wan et al. [6], different resonator systems such as 1D parity-time-symmetric structure [7], ring cavities [8], were proposed and studied. Nevertheless, in practice the refractive index of a general resonator, like the uniform slab, is a fixed value for a given incident wavelength and difficultly happen to satisfy the CPA conditions. To solve this problem, more recently, grating structure instead of uniform slab for CPA is proposed by Shen et al. [9]. It shows that a grating structure can generally exhibit time-reversed lasing better than a uniform slab and can even realize time-reversed lasing for any incident wavelength by adjusting the grating geometric parameters. Particularly, significant absorption can be achieved in a broad frequency range in grating structure. On the other hand, the terahertz (THz) wave, whose frequency lies between the microwave and infrared light, is one of the least-explored areas in the electromagnetic spectrum [10]. Due to great potential in the fields

including communication, imaging, biological diagnosis, and chemical analysis [11–13], THz science and technology have received rapidly growing attention so far. Some related THz functional devices, such as switches [14,15], filters [16], waveguides [17,18], modulators [19], perfect absorbers [20], and polarization components [21], have been also greatly developed. However, THz components based on new concepts are still critically needed [22,23].

In term of these, here we extend the CPA research from conventional visible region to the THz region. We demonstrate that both uniform slab and grating can support THz time-reversed lasing. Comparatively, a grating is more effective than a uniform slab due to its tunable effective refractive index, and can also offer significant absorption in a broader frequency range. Furthermore, the applications of THz time-reversed lasing for novel concentration/thickness sensors are preliminarily explored in a single-channel CPA system.

2. Design and theory

Fig. 1(a) shows the general schematic of a two-channel CPA system constructed by uniform slab with refractive index $n = n_{\mathrm{Re}} + i n_I$ ($n_{\mathrm{Re}} > 1$, $n_I > 0$) and thickness d. As discussed in Refs. [5] and [9], for such uniform slab surrounded by dielectric with refractive index n_0, the CPA condition of having a zero eigenvalue is $e^{inkd} = \pm (n - n_0)/(n + n_0)$, where k is the wave number in vacuum. Assuming that $n_I \ll n_{\mathrm{Re}}$, the CPA zero solution of this equation is approximately

$$n_{\mathrm{Re},m} \approx m\pi /(kd) \quad (m = 1, 2, 3, \ldots), \qquad (1)$$

* Corresponding author. Fax: +86 791 83969238.
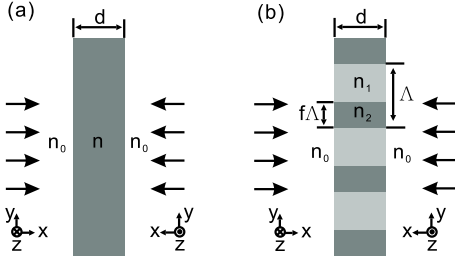E-mail address: shenyunoptics@gmail.com (Y. Shen).

Fig. 1. (Color online.) Schematic of (a) uniform slab with refractive index n and (b) grating structure consisting of alternating layers with refractive indices n_1 and n_2. In (b), Λ and f are severally the period and filling factor. In (a) and (b), d is the thickness, n_0 is the refractive index of surrounding dielectric.
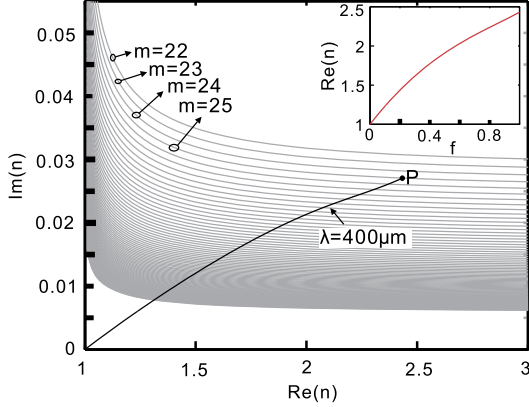

Fig. 2. (Color online.) Relations of Im(n) and Re(n). Gray solid curves represent the relations deduced from Eq. (2) and denote CPA zero solutions. Black solid curve represents the trajectory of n_{eff} of NaCl/air grating for 400 μm incident light as f varies from 0 to 1. The refractive index of NaCl for 400 μm is marked as point P. Inset: dependence of Re(n) of n_{eff} on f for 400 μm incidence.

and $n_{I,m} \approx 1/(kd)\ln[(n_{Re,m} + n_0)/(n_{Re,m} - n_0)]$. Then the relations of $n_{Re,m}$ and $n_{I,m}$ can be further deduced as

$$\frac{n_{I,m}}{n_{Re,m}} = \frac{\ln[(n_{Re,m} + n_0)/(n_{Re,m} - n_0)]}{m\pi} \quad (m = 1, 2, 3, \ldots). \quad (2)$$

Accordingly, to enable time-reversed lasing, n_{Re} and n_I of the slab must satisfy the CPA condition (2), and thickness d of the slab must be concurrently chosen to meet the CPA condition (1). Here, the condition (2) is a prerequisite and can be expressed by graph. For $n_0 = 1$, it is illustrated in Fig. 2 with gray solid curves, where a range of m from 22 to 107 is displayed.

Nevertheless, in practice the complex refractive index n of a uniform slab for a given incident wavelength may be difficult to fall exactly on the CPA zero curves in Fig. 2 to meet the CPA condition (2), but locates within the spacing of them. To solve this problem, a grating structure shown in Fig. 1(b) instead of the uniform slab for CPA is proposed by Shen et al. [9]. It is shown that in a grating structure, the effective refractive index n_{eff} can be flexibly tuned by filling factor to artificially fall on CPA zero curves to meet CPA condition. Thus, time-reversed lasing can be exhibited even for any incident wavelength by choosing proper grating geometric parameters. Moreover, compared with uniform slab, significant absorption can also be achieved in a broad frequency range for the grating structure. Specifically, for a typical grating structure consisting of alternating dielectric layers with refractive indices n_1 and n_2 shown in Fig. 1(b), when period Λ is much smaller than the wavelength of incident light λ, the grating can be treated as a uniform slab with effective refractive index n_{eff} which can be evaluated with the effective medium theory (EMT) [9,24,25]. In Fig. 2(b), d is grating thickness; f is filling factor defined as the ratio of length of layer n_2 to grating period. Considering normal

incidence of TE polarization light on the grating, n_{eff} can be described by the EMT in the second-order approximation as

$$n_{eff} = \sqrt{(1-f)n_1^2 + fn_2^2 + \frac{\pi^2}{3}\left(\frac{\Lambda}{\lambda}\right)^2 f^2(1-f)^2\left(n_2^2 - n_1^2\right)^2}. \quad (3)$$

From Eq. (3) we can know, when f grows from 0 to 1, n_{eff} will vary from n_1 to n_2. Hence, if air with $n = 1$ and a ordinary medium with Re(n) > 1 and Im(n) > 0 are severally chosen for layer n_1 and n_2 in Fig. 1(b), the trajectory of n_{eff} from point $(0, 1)$ of n_1 to point $[\text{Re}(n_2), \text{Im}(n_2))]$ of n_2 must have cross points with the CPA zeros curves in Fig. 2 as long as m is large enough. Then, by controlling f to make n_{eff} fall on the cross points, CPA condition (3) can be artificially satisfied and support time-reversed lasing.

3. Simulation and discussion

To demonstrate time-reversed lasing in the THz frequency range, we now severally choose uniform Sodium Chloride (NaCl) [26] slab and NaCl/air grating as instances, and their properties of scattering coefficient S around incident wavelength $\lambda = 400$ μm (corresponding to 0.7495 THz) are investigated. Here, the S is defined as the ratio of the scattered and input intensities. Typically, the scattered intensity of a uniform slab/grating near a CPA zero has $I \sim c_0|n - n_{CPA,m}|^2$, where c_0 is of order unity, and $n_{CPA,m} = n_{Re,m} + in_{I,m}$ is the CPA zero solutions [see Eq. (2), and Fig. 2, gray solid curves]. As discussed in Ref. [9], we can take suitable d [see Eq. (1)] that make $n_{Re,m} \approx n_{Re}$ and optimal m that let $|n_I - n_{I,m}|$ be the smallest to provide the minimum of $|n - n_{CPA,m}|$ and S, while $S \approx 0$ implies the time-reversed lasing. Generally, if n lies within the spacing between CPA zeros curves in Fig. 2, the minimum of $|n - n_{CPA,m}|$ and S won't be zero in any way. Nevertheless, in grating structure we can use controllable effective refractive index n_{eff} instead of n and artificially tune it to locate on CPA zeros curves, making $|n - n_{CPA,m}|$ and S be zero. Here, for uniform NaCl slab, as the refractive index of NaCl [26] for 400 μm incidence is $n = 2.43 + 0.027i$ (marked as point P in Fig. 2) happens to locate near CPA zero curve of $m = 25$, we can take the suitable thickness $d = 2057.61$ μm to make $n_{Re,25} = 2.43$ in Eq. (1). With this thickness, the S around $\lambda = 400$ μm is calculated and plotted in Fig. 3 with red solid curve. The curve on logarithmic scale is also shown in Fig. 3 inset with red solid curve. In the calculation, practical refractive indices of NaCl for all 350–450 μm are performed. From the red solid curves we can see that CPA is realized near $\lambda = 400$ μm. However, the significant absorption cannot be efficient enough' through the whole operating frequency of 350–450 μm, and the upper limit of S reaches to 0.5181 at 416.7 μm. In the same way, we now consider the example of NaCl/air grating surrounded by air with $\Lambda = 84.14$ μm. For $\lambda = 400$ μm, the n_{eff} can be tuned between 1 and $2.43 + 0.027i$ by controlling the filling factor f according to Eq. (3), and the trajectory of n_{eff} is shown with black solid curve in Fig. 2, which intersects all gray curves of $m > 25$. In Fig. 2 inset, the relation of the real part of n_{eff} and f is presented. Evidently, we can artificially tune n_{eff} to locate at the cross points of the trajectory and mth CPA zero curve to make CPA condition of Eq. (2) perfectly satisfied and support perfect time-reversed lasing. For instance, we can choose $f = 0.5$ to make $n_{eff} = 1.916 + 0.202i$ locating at the cross point of the trajectory and CPA zero curve of $m = 35$. Under such grating geometric parameters, the S around $\lambda = 400$ μm is calculated and illustrated in Fig. 3 with gray dotted curve. Here, suitable grating thickness $d = 3653.40$ μm is chosen to let $n_{Re,35} = 1.916$ in Eq. (1) be satisfied. Furthermore, as $f = 0.194$ is chosen with $n_{eff} = 1.4273 + 0.0105i$ and $m = 75$, S is depicted in Fig. 3 with blue dashed curve. The curves above on logarithmic scale are severally shown in Fig. 3 inset. We can see that in